Journal of
Mechanics of
Materials and Structures

REPRESENTATIVE VOLUME ELEMENT AND EFFECTIVE ELASTIC PROPERTIES OF OPEN CELL FOAM MATERIALS WITH RANDOM MICROSTRUCTURES

Sergey Kanaun and Oleksandr Tkachenko

Volume 2, № 8 October 2007

mathematical sciences publishers

JOURNAL OF MECHANICS OF MATERIALS AND STRUCTURES
Vol. 2, No. 8, 2007

REPRESENTATIVE VOLUME ELEMENT AND EFFECTIVE ELASTIC PROPERTIES OF OPEN CELL FOAM MATERIALS WITH RANDOM MICROSTRUCTURES

SERGEY KANAUN AND OLEKSANDR TKACHENKO

This work is devoted to the problem of the numerical simulation of effective elastic properties of open-cell foam materials. The Laguerre tessellation procedure is used for the construction of skeletons of random foam microstructures with prescribed distributions of cell diameters. A four-parametric approximation of the ligament shapes in the open-cell foams is proposed. A version of the finite element method, based on the Timoshenko beam finite element, is developed for calculating stresses and strains in the foam ligaments and the solution of the homogenization problem. The size of the representative volume element for reliable calculations of the effective elastic properties of the foam materials is evaluated on the basis of a series of numerical experiments. The dependences of the effective elastic properties of the open-cell foams on cell size distributions and on ligament shapes are obtained and analyzed.

1. Introduction

Physical and mechanical properties of carbon foam materials have been extensively studied in recent decades. Interest in these very light and highly thermoconductive materials has increased because of many important areas of their applications. A typical microstructure of the open-cell foams is shown on the left-hand side of Figure 1. It consists of a set of ligaments (fiber like elements) connected to a number of nodes that are, in fact, irregular lumps. The cross section of a typical ligament is presented on the right-hand side of Figure 1. For applications, it is important to predict the dependence of a foam material's mechanical and physical properties on the details of its microstructure. Effective elastic properties of foam-like systems have been studied by many authors [Gibson and Ashby 1982; Warren and Kraynik 1997; Christensen 2000; Roberts and Garboczi 2002; Gong et al. 2005]. Analytical equations for the Young moduli and the Poisson ratios of such materials were obtained for regular structures, and approximation of an actual random foam structure by a regular one allows us to describe experimental behavior of the effective elastic properties of such materials in some region of microstructural parameters [Gong et al. 2005]. Nevertheless, in the framework of the regular approach, many important details of mechanical and physical behavior of random foams cannot be described (see discussions of this problem in Roberts and Garboczi [2002] and Zhu et al. [2000]).

In the works of Roberts and Garboczi [1999; 2001; 2002], Zhu et al. [2000], and Kadashevich and Stoyan [2005], elastic properties of the open-cell foams by direct numerical simulations of the elastic

Keywords: open-cell foams, representative volume element, random space tessellation, homogenization problem, finite element method, elastic constants.

This work was supported by the Texas A& M University (USA) and CONACYT (Mexico) joint program (Proposal 3-050102-1), and AFSOR (Grant FA9550-06-1-0347).

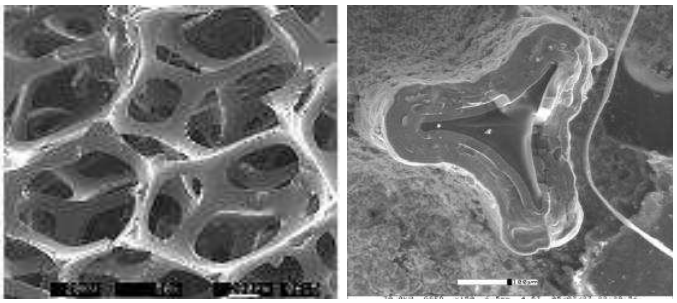

Figure 1. Scanning electron microscopy image of an open-cell carbon foam microstructure (left), and the cross section of a typical ligament (right).

fields inside a representative volume element (RVE) of the foam material. The process of numerically simulating the effective elastic properties of open-cell foams consists of the following steps: First, the microstructure (skeleton) of the foam material is constructed using statistical models of the actual foam microstructure. As a rule, the Voronoii tessellation procedure is used to produce a set of polyhedron cells inside the chosen RVE. The geometry of the open-cell foam in the RVE is defined by using the edges of the Voronoii polyhedra as the axes of the ligaments, and by choosing a certain approximation of the ligament shapes. Next, the finite element technique is applied for calculation of stresses and strains in the ligaments for given boundary conditions on the surface of the RVE. Finally, the values of the effective elastic constants of the foam are obtained by averaging detailed strain and stress fields over the RVE.

The first problem that must be addressed in carrying out numerical simulations is the appropriate choice of RVE size. If the RVE is a cube, one has to point out the number of cells that should be taken inside this cube by the numerical simulations in order to obtain reliable values for the effective elastic constants of the foam material. Usually, the number of cells in the RVE is restricted by capacities of available computers and software. Standard finite element packages permit the consideration of RVEs that contain hundred of cells. Nevertheless, in some works (see [Kadashevich and Stoyan 2005]) the authors came to the conclusion that the number of cells in the RVE should be more than a thousand in order to obtain reliable values of the effective elastic constants.

Another problem that must be addressed in carrying out numerical simulations of the effective properties of foams is the construction of the foam microstructures with the law of the cell size distribution that corresponds to the one observed in the actual foams. In fact, the Voronoii tessellation procedure does not permit the simulation of microstructures with predetermined distributions of the cell sizes. To be exact, it is impossible to point out the positions of seed points in the RVE that produce the Voronoii polyhedra with the prescribed distribution of diameters.

The influence of ligament shape on the properties of open-cell foams is another important problem that has not been considered sufficiently in the literature. The ligaments in the actual foams have rather complex geometry. An adequate description of this geometry, and an analysis of its influence on the effective properties, are important tasks of numerical simulations.

The paper is focused on the above-mentioned problems, and its structure is as follows:

(1) In Section 2, the problem of computer simulation of skeletons of the open-cell foams is considered. We use the Voronoii and Laguerre tesselation procedures in order to construct a set of cells inside

a cubic RVE. The Laguerre procedure allows us to simulate foam skeletons with a given known distribution of cell diameters.

(2) In Section 3, an analytical four-parametric approximation of the ligament form is proposed. This approximation reflects the most important features of the ligaments in actual foams.

(3) In Section 4, a version of the finite element method based on the Timoshenko beam theory is developed for calculation of stresses and strains in the ligaments of the open-cell foam structures. In this method, every ligament is considered as one finite element (super element), and it results that the RVE with several thousands of cells may be considered. The appropriate size of the cubic RVE is assessed in Section 5. Performing series of numerical experiments we show that the number of cells in the RVE should be about 900–1000 in order to obtain reliable values of the effective elastic constants of the open-cell foams.

(4) The influence of the ligament form and the cell size distribution on the effective elastic properties of foams is studied in Section 6. Some details of the proposed method and its possible area of application are discussed in the conclusion.

2. Computer simulation of skeletons of open-cell foam materials

A conventional method for carrying out computer simulations of the microstructures of open-cell foams, shown in Figure 1, is based on the Voronoii tessellation algorithm. In our study, this algorithm is used in the following specific form. Let us consider a cube $V : \{|x_1| < 1, |x_2| < 1, |x_3| < 1\}$ centered at the origin of the Cartesian coordinate system, (x_1, x_2, x_3). First, a random set $S_{(0,0,0)}$ of the so-called seed points, homogeneously distributed inside this cube, is generated. After that, the sets $S_{(i,j,k)}$ $(i, j, k = 0, \pm 1)$ that have mirror-like symmetry to the set $S_{(0,0,0)}$ with respect to the planes $x_i = \pm 1$ $(i = 1, 2, 3)$, are constructed. For instance, the set $S_{(1,0,0)}$ is mirror-like to the set $S_{(0,0,0)}$ with respect to the plane $x_1 = 1$, the set $S_{(0,1,0)}$ is symmetric to the set $S_{(0,0,0)}$ with respect to the plane $x_2 = 1$, etc. The union of these sets $\bar{S} = S_{(0,0,0)} \cup S_{(1,0,0)} \cup \ldots \cup S_{(0,0,-1)}$ is the set of seed points under consideration. The Voronoii polyhedron that corresponds to a seed point $x^{(i)}$ with the coordinates $(x_1^{(i)}, x_2^{(i)}, x_3^{(i)})$ consists of the points of three-dimensional space that are closer to the point $x^{(i)}$ than to any other seed point $x^{(j)}$. The Voronoii polyhedra that correspond to the seed points of the set $S_{(0,0,0)}$ perform a tesselation of the original cube V. Because of the mirror symmetry of the sets $S_{(i,j,k)}$ $(i, j, k = 0, \pm 1)$ with respect to $S_{(0,0,0)}$, the borders of the cube V belong to the polyhedron surfaces. For the realization of the Voronoii tesselation procedure, the algorithm proposed by Tenemura et al. [1983] was adopted in this work.

A typical polyhedron obtained by the Voronoii tessellation procedure is shown in Figure 2. The edges of this polyhedron compose the ligament axes of the future foam microstructure, and the polyhedron vertices are the nodes where the ligaments are connected. Note that very often the Voronoii tessellation produces polyhedra whose vertices are situated too closely to each other (e.g. the set A of nodes in Figure 2), and the lengths of the ligaments that connect these close nodes are very short. Because every ligament has a finite volume, these short ligaments turn out to be inside other ligaments that connect more distant nodes. It means that the obtained tessellation model should be altered (cleaned): the clusters of the nodes that are closer to each other than a characteristic size of the ligament cross-sections should be joined into one node. An additional reason for such a procedure is that the elastic deformation of very short ligaments

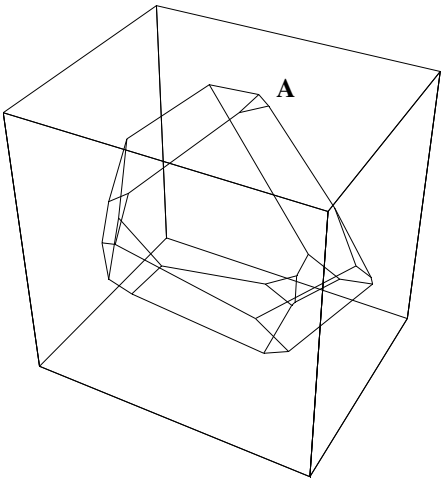

Figure 2. A typical polyhedron obtained by the Voronoii 3D-space tesselation process.

cannot be described by the beam theory that is used in the finite element technique adopted in this study (Section 4). If the number of such short ligaments is large, the error of the calculation of elastic fields based on the beam finite elements may be essential.

In Figure 3, the Voronoii tessellation of a cube with two hundred cells is presented. The seed points corresponding to these structure were homogeneously distributed inside the cube under an additional condition that the distance between two different points $x^{(i)}$ and $x^{(j)}$ should be more than 0.3. The

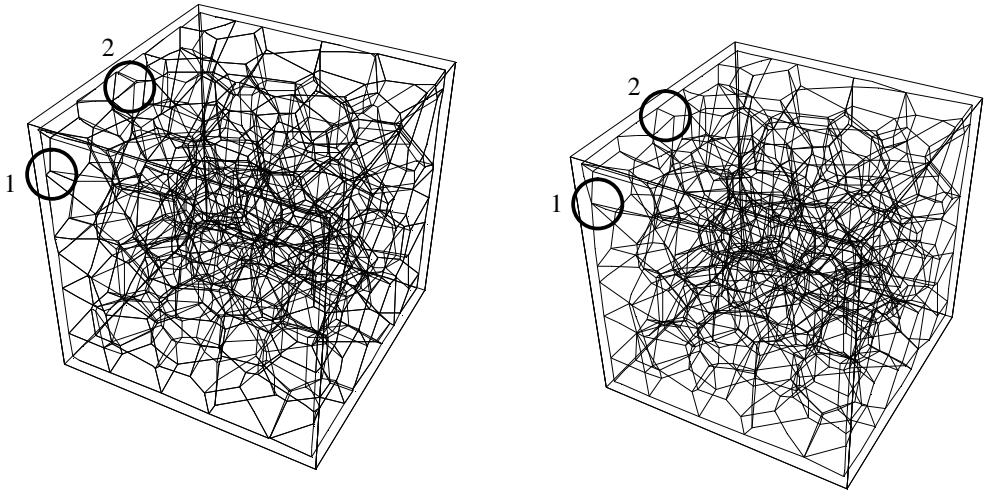

Figure 3. The Voronoii tesselation of the cube (left) and the same structure after elimination of two small polyhedron surfaces (right). (In the regions 1 and 2 in the right picture, small polyhedron surfaces are eliminated).

images of the tessellation before and after the "cleaning" procedure are presented in the left and right hand sides of Figure 3. In the right hand side of Figure 3, the nodes that are closer than 0.05 are joined into one node. If the original left hand side structure consists of 3855 ligaments with the maximal and minimal lengths 0.5559 and $1.26 \cdot 10^{-6}$ and the mean length 0.138, the final structure contains 1971 ligaments of the maximal and minimal lengths 0.557 and 0.05, and the mean ligament length is equal to 0.205. The difference between two microstructures may be observed in regions 1 and 2 in the left and right hand sides of Figure 3.

The distribution function $f(d)$ of the diameters d of the cells shown in Figure 3 is presented in Figure 4. Note that this distribution is difficult to control in the framework of the Voronoii tessellation procedure. In actual carbon foam materials, however, the cell size distributions are rather specific. In many cases, the experimental histograms of the cell diameters are close to a linear distribution law: $f(d) \approx ad$, where a is an appropriate constant (K. Lafdi, 2004, private communication). The diameter d of a cell is calculated from the equation $d = 2\sqrt[3]{3v/(4\pi)}$, where v is the volume of the cell.

For simulation of the microstructure of the foam materials with a prescribed distribution of cell diameters, the so-called Laguerre tesselation procedure may be used. The application of this procedure consists of two steps. First, a set of balls of random diameters $d^{(i)}$, whose distribution coincides with the distribution of cell diameters of the simulated foam, is generated. After that, these balls are closely packed inside the RVE (cube V). As a result, we obtain a set of ball centers $x^{(i)}$ and a set of diameters $d^{(i)}$ associated with these centers. Next, this information is used for the Laguerre tesselation of the cube V. Following Aurenhammer and Klein [2000], let us consider a ball $B^{(i)}$ of the diameters $d^{(i)}$ centered at the point $x^{(i)}$. A positive scalar $t(x^{(i)}, x)$,

$$t(x^{(i)}, x) = \sqrt{|x^{(i)} - x|^2 - \left(\frac{d^{(i)}}{2}\right)^2}, \tag{1}$$

is the distance from a point x ($x \notin B^{(i)}$) to the surface $S^{(i)}$ of $B^{(i)}$ along the tangent line to this surface (see Figure 5). The ith Laguerre polyhedron consists of the union of the points of the ith ball and the points x for which the parameter $t(x^{(i)}, x)$ is less than such a parameter $t(x^{(j)}, x)$ for any other jth ball,

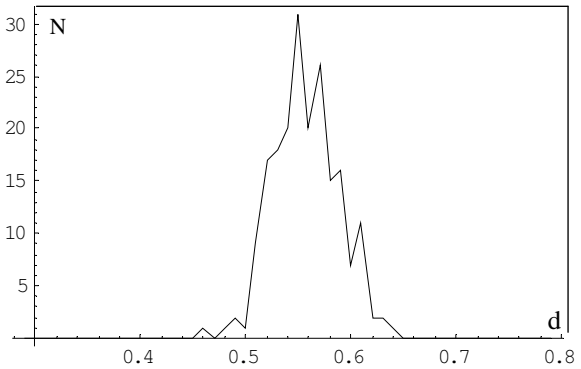

Figure 4. A typical histogram of the cell diameters obtained after the Voronoii tessellation process.

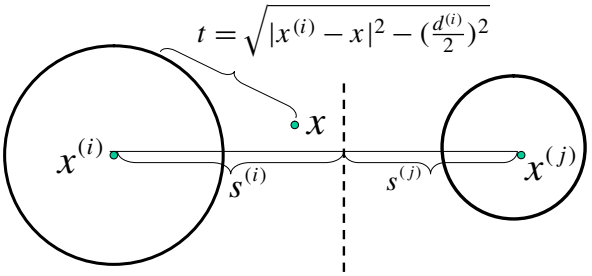

Figure 5. The Laguerre tesselation algorithm; the point x belongs to the ith Laguerre polyhedron if the parameter t is smaller for the point $x^{(i)}$ then for any other seed point $x^{(j)}$.

$i \neq j$. It is possible to show that the common border of the Laguerre polyhedron that correspond to two neighbor balls i and j centered at the points $x^{(i)}$ and $x^{(j)}$, $|x^{(i)} - x^{(j)}| \geq (d^{(i)} + d^{(j)})/2$, is orthogonal to the interval connecting the centers of these balls, and that the border plane intersects this interval in the proportion $s^{(i)}/s^{(j)}$,

$$\frac{s^{(i)}}{s^{(j)}} = \frac{4|x^{(i)} - x^{(j)}|^2 + \left(d^{(i)}\right)^2 - \left(d^{(j)}\right)^2}{4|x^{(i)} - x^{(j)}|^2 + \left(d^{(j)}\right)^2 - \left(d^{(i)}\right)^2}. \tag{2}$$

The intervals $s^{(i)}$ and $s^{(j)}$ are indicated in Figure 5, and the dashed line in this figure is the border of the Laguerre polyhedra. It is shown in [Aurenhammer and Klein 2000] that all Laguerre polyhedra are convex and span three-dimensional space.

The algorithm of packing used in this work is based on the following procedure. We start with the first ball centered at the origin, and the center $x^{(i)}$ of the ith ball is defined such that $x^{(i)}$ has minimal distance from the center of the cube, and $|x^{(i)} - x^{(j)}| \geq (d^{(i)} + d^{(j)})/2$ for $j = 1, 2, 3, \ldots, i-1$. The number of the balls is increased until it is impossible to find a center for the next ball inside the cube.

The algorithm of Tenemura et al. [1983] is also adopted for carrying out the Laguerre tesselation procedure.

Figure 6 presents the histograms of three distribution functions $f(d)$ of the diameters of the Laguerre polyhedra for different distributions of the diameters of the initial balls. The line with black rhombs corresponds to a set of balls of approximately the same diameters, the line with triangles corresponds to a homogeneous distribution of the ball diameters in the region $(0.5\,\langle d\rangle\,,\,1.5\,\langle d\rangle)$, and the line with squares corresponds to a linear distribution of the ball diameters in the interval $(0.3\,\langle d\rangle\,,\,1.2\,\langle d\rangle)$. Here $\langle d\rangle$ is the mean value of the ball diameters.

3. Approximation of the form a typical ligament in the open-cell foams

As seen from Figure 1, the cross-section of a typical ligament has a quasitriangular form (see also the discussion of the forms of ligaments in carbon foams in [Gong et al. 2005]). In this study, we treat a typical ligament as a direct beam with a quasitriangular cross-section that changes along the ligament

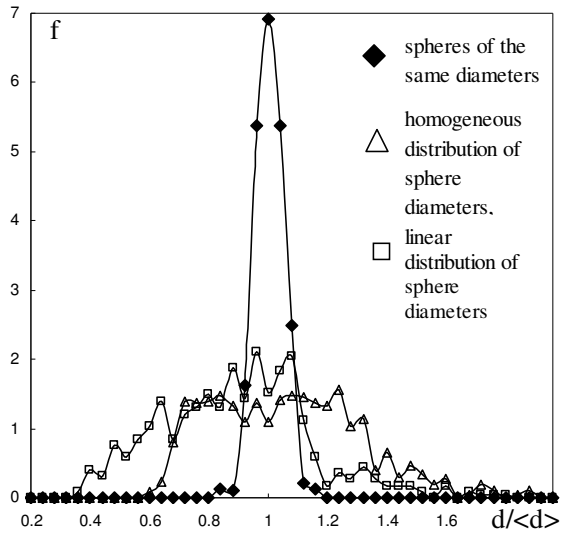

Figure 6. The distribution function of cell diameters after the Laguerre tesselation for random packing of spheres of approximately the same diameter (line with black rhombs), for packing of spheres with the homogeneous distribution of the diameters in the interval $\{0.5\,\langle d\rangle\,,\,1.5\,\langle d\rangle\}$ (line with triangles), and for packing of spheres with linear distribution of diameters on the interval $\{0.3\,\langle d\rangle\,,\,1.2\,\langle d\rangle\}$ (line with squares).

axis. Taking into account that function $f(\zeta)$ of a complex variable ζ,

$$f(\zeta) = R\left(\frac{1}{\zeta} + \frac{\zeta^2}{a_1}\right), \qquad a_1 \geq 2,$$

maps a unit circle in the ζ-plane into a quasitriangular region in the $w = f(\zeta)$-plane, we define the border of the ligament cross-section by the equations

$$\begin{aligned} y(\varphi, x) &= R(x)\left(\cos(\varphi) + \frac{\cos(2\varphi)}{a_1}\right), \\ z(\varphi, x) &= R(x)\left(-\sin(\varphi) + \frac{\sin(2\varphi)}{a_1}\right). \end{aligned} \tag{3}$$

Here φ is the angle parameter, $0 \leq \varphi < 2\pi$, (y, z) are the Cartesian coordinates in the plane of the ligament cross-section, and the coordinate x is directed along the ligament axis. The function $R(x)$ that defines the change of the ligament along its axis is taken in the form

$$R(x) = a_2\left[1 - a_3\xi(1-\xi)\right], \qquad \xi = \frac{x}{l}, \qquad 0 < x < l, \tag{4}$$

which reflects the experimental fact that the ligaments are thinner in the middle region than in the regions near their ends: $x = 0, l$.

Parameters a_1, a_2, a_3 and l define the global shape of the ligament. The cross-sections of the ligament by the plane $x_3 = 0$ is presented in Figure 7 for the parameters $a_2 = 0.3$ and $a_1 = 2, 3, 10$. The shape

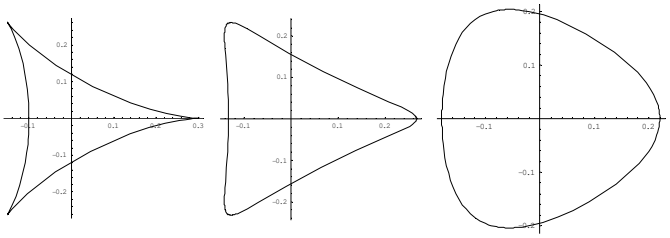

Figure 7. Ligament cross-sectional area different values of the parameter a_1 in Equation (3), $a_2 = 0.3$, $\xi = 0$.

of a typical ligament that corresponds to Equation (3) and Equation (4) is presented in Figure 8 for the parameters $a_1 = 2.5$, $a_2 = 0.3$, $a_3 = 0.4$.

The proposed approximation allows us to calculate the basic geometrical characteristics of the ligament in closed analytical form. For instance, the area S of the cross-section of the ligament is

$$S(a_1, a_2, a_3, \xi) = \pi a_2^2 \frac{(a_1^2 - 2)}{a_1^2} \left[1 - 4a_3^2 \xi(1 - \xi)\right]^2. \tag{5}$$

The main moment of inertia J of the cross-section takes the form

$$J(a_1, a_2, a_3, z) = \pi a_2^4 \frac{(a_1^4 - 2a_1^2 - 2)}{4a_1^4} \left[1 - 4a_3^2 \xi(1 - \xi)\right]^4. \tag{6}$$

The volume V_l of the ligament is

$$V_l(a_1, a_2, a_3) = \pi a_2^2 l \frac{(a_1^2 - 2)}{15a_1^2}(15 - 20a_3 + 8a_3^2). \tag{7}$$

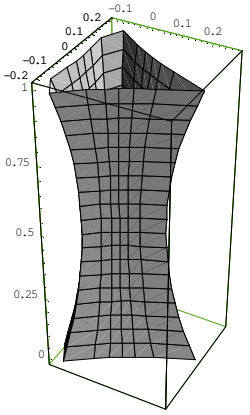

Figure 8. The shape of a ligament defined by Equations (3) and (4) for $a_1 = 2.5$, $a_2 = 0.3$, $a_3 = 0.4$.

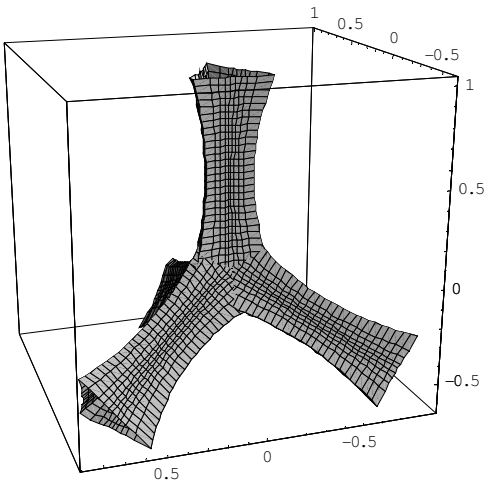

Figure 9. A typical node of the foam structure where four ligaments intersect.

A typical element of the microstructure of the foam material consists of four ligaments connected in a node. Such an element is shown in Figure 9. For calculating the volume of the hard phase in the RVE, one has to take into account the volume V_{int} of the intersection of the ligaments in the nodes. The volume V_{int} may be evaluated approximately as the sum of four pyramids with bases of area S_{int} , and we can write

$$S_{int} = S(a_1, a_2, a_3, \frac{a_2}{l}), \qquad V_{int} = \frac{4}{3} a_2 S_{int}. \tag{8}$$

Here the function $S(a_1, a_2, a_3, \xi)$ is defined in Equation (5). Finally, the volume V_h of the hard phase in the RVE may be evaluated from the equation

$$V_h = N_l V_{l-2a_2} + N_n V_{int}.$$

Here N_l is the number of the ligaments, N_n is the number of the nodes in the RVE, V_{l-2a_2} is the volume of the ligament without two zones of length a_2 near its ends

$$V_{l-2a_2} = \pi a_2^2 l \frac{(a_1^2 - 2)}{15 a_1^2}(1-2\lambda)[15 + 4a_3(2a_3 - 5) - 8a_3(1-\lambda)\lambda\,(5 - 2a_1 - 6a_1\lambda(1-\lambda))], \qquad \lambda = \frac{a_2}{l}.$$

Thus, the geometrical structure of the open-cell foam inside a cubic region V is defined if the coordinates of all the nodes and connections between them are indicated as well as the parameters a_1, a_2, a_3 of all the ligaments that perform such connections.

4. The finite element method

The version of the finite element method used in this work for calculating elastic fields in the ligaments of open-cell foams is based on a special beam element. The geometry of a typical beam was described in the previous section, and its material is assumed to be elastic with a Young modulus E and Poisson ratio ν. The Timoshenko beam model is used to describe the deformation of the beam element.

Let us consider a beam element of length l, and introduce a local Cartesian coordinate system (x, y, z) with the origin at the left end of the beam and the x-coordinate directed along the beam axis. The ends of the beam (nodes) are labeled with numbers 1 and 2. The vectors of the nodal displacements $\{u_x^{(i)}, u_y^{(i)}, u_z^{(i)}\}$ and rotations $\{\theta_x^{(i)}, \theta_y^{(i)}, \theta_z^{(i)}\}$ compose the generalized vector of displacements

$$\mathbf{d}^{(i)} = \{u_x^{(i)}, u_y^{(i)}, u_z^{(i)}, \theta_x^{(i)}, \theta_y^{(i)}, \theta_z^{(i)}\}^T$$

of the ith node $(i = 1, 2)$. The two vectors $\left\{\mathbf{d}^{(1)}, \mathbf{d}^{(2)}\right\}^T$ completely define the deformation of the beam. Hence, the degrees of freedom per node are equal to 6 (3 displacements and 3 rotations). The vectors of the nodal forces $\{f_x^{(i)}, f_y^{(i)}, f_z^{(i)}\}$ and moments $\{m_x^{(i)}, m_y^{(i)}, m_z^{(i)}\}$ compose the vector of generalized force $\mathbf{p}^{(i)} = \{f_x^{(i)}, f_y^{(i)}, f_z^{(i)}, m_x^{(i)}, m_y^{(i)}, m_z^{(i)}\}^T$. Here $\{\}^T$ is the transposed vector.

We derive the beam stiffness matrix by using the direct method of Cook et al. [1989]. The stiffness matrix $\mathbf{K}$ of the beam element is defined by the equation

$$\mathbf{K}\begin{Bmatrix}\mathbf{d}^{(1)}\\ \mathbf{d}^{(2)}\end{Bmatrix} = \begin{Bmatrix}\mathbf{p}^{(1)}\\ \mathbf{p}^{(2)}\end{Bmatrix}, \qquad \mathbf{K} = \begin{bmatrix}\mathbf{K}_{11} & \mathbf{K}_{12}\\ \mathbf{K}_{21} & \mathbf{K}_{22}\end{bmatrix}. \tag{9}$$

Here $\mathbf{K}_{ij}$ are the block elements of the stiffness matrix that are constructed below. There are two vector equations of equilibrium connecting the nodal forces and moments:

$$\begin{aligned}\mathbf{p}^{(1)} + \mathbf{R}_{12}\mathbf{p}^{(2)} &= \{\mathbf{0}\},\\ \mathbf{R}_{21}\mathbf{p}^{(1)} + \mathbf{p}^{(2)} &= \{\mathbf{0}\},\end{aligned} \tag{10}$$

where matrices $\mathbf{R}_{12}$ and $\mathbf{R}_{21}$ have forms

$$\mathbf{R}_{12} = \begin{bmatrix} 1 & 0 & 0 & 0 & 0 & 0\\ 0 & 1 & 0 & 0 & 0 & 0\\ 0 & 0 & 1 & 0 & 0 & 0\\ 0 & 0 & 0 & 1 & 0 & 0\\ 0 & 0 & L & 0 & 1 & 0\\ 0 & -L & 0 & 0 & 0 & 1 \end{bmatrix}, \qquad \mathbf{R}_{21} = \begin{bmatrix} 1 & 0 & 0 & 0 & 0 & 0\\ 0 & 1 & 0 & 0 & 0 & 0\\ 0 & 0 & 1 & 0 & 0 & 0\\ 0 & 0 & 0 & 1 & 0 & 0\\ 0 & 0 & -L & 0 & 1 & 0\\ 0 & L & 0 & 0 & 0 & 1 \end{bmatrix}, \qquad \mathbf{R}_{12} = \mathbf{R}_{21}^{-1}.$$

The strain energy U of the Timoshenko beam can be expressed as follows [Pilkey et al. 2003]

$$U = \frac{1}{2}\left(\int_0^L \frac{N^2(x)}{ES(x)}\,dx + \int_0^L \frac{M_y^2(x)}{EJ(x)}\,dx + \int_0^L \frac{M_z^2(x)}{EJ(x)}\,dx\right) + \frac{1}{2}\left(\int_0^L \frac{M_x^2(x)}{\mu\widehat{J}_p(x)}\,dx + \int_0^L \frac{\alpha_s V_y^2(x)}{\mu S(x)}\,dx + \int_0^L \frac{\alpha_s V_z^2(x)}{\mu S(x)}\,dx\right),$$

where S, J are the area and the main moment of inertia of the beam cross-section, respectively (see Section 3), $\widehat{J}_p$ is the corrected polar moment of inertia that results from the solution of the torsion problem for a beam with a noncircular cross section

$$\widehat{J}_p = \pi a_2^4(1 - 4a_1^{-2} + 2a_1^{-4})(1 - 4a_3^2\xi(1-\xi))^4,$$

and α_s is the shear deformation coefficient [Pilkey et al. 2003, p. 750]. F_x , F_y , F_z are internal axial and shear forces, M_x , M_y , M_z are internal torque and bending moments.

Let us fix displacements at node 2 ($\mathbf{d}^{(2)}=\mathbf{0}$) and apply the force $\mathbf{p}^{(1)}$ to node 1. In this case, the internal forces in the beam are

$$\begin{aligned} F_x(x) &= -f_x^{(1)}, & F_y(x) &= -f_y^{(1)}, & F_z(x) &= -f_z^{(1)}, \\ M_x(x) &= -m_x^{(1)}, & M_y(x) &= -m_y^{(1)} - f_z^{(1)}x, & M_z(x) &= -m_z^{(1)} + f_y^{(1)}x. \end{aligned} \tag{11}$$

The Castigliano theorem$\left(\frac{\partial U}{\partial \boldsymbol{p}} = \mathbf{d}\right)$ together with equilibrium Equation (10) give us the equations

$$\mathbf{S}_{11}\mathbf{p}^{(1)} = \mathbf{d}^{(1)}, \qquad \mathbf{R}_{21}\mathbf{p}^{(1)} + \mathbf{p}^{(2)} = \{\mathbf{0}\}, \tag{12}$$

where $\mathbf{S}_{11}$ is the flexibility matrix

$$\mathbf{S}_{11} = \begin{bmatrix} s_{11} & 0 & 0 & 0 & 0 & 0 \\ 0 & s_{22} & 0 & 0 & 0 & -s_{26} \\ 0 & 0 & s_{33} & 0 & s_{35} & 0 \\ 0 & 0 & 0 & s_{44} & 0 & 0 \\ 0 & 0 & s_{35} & 0 & s_{55} & 0 \\ 0 & -s_{26} & 0 & 0 & 0 & s_{66} \end{bmatrix}. \tag{13}$$

The components s_{ij} of this matrix are defined by the equations

$$\begin{aligned} s_{11} &= \frac{L}{E}\int_0^1 \frac{1}{S(\xi)}d\xi, & s_{22} = s_{33} &= \frac{L^3}{E}\int_0^1 \frac{\xi^2}{J(\xi)}d\xi + \frac{\alpha_s L}{\mu}\int_0^1 \frac{1}{S(\xi)}d\xi, \\ s_{44} &= \frac{L}{\mu}\int_0^1 \frac{1}{\widehat{J}_p(\xi)}d\xi, & s_{55} = s_{66} &= \frac{L}{E}\int_0^1 \frac{1}{J(\xi)}d\xi, \\ s_{35} &= \frac{L^2}{E}\int_0^1 \frac{\xi}{J(\xi)}d\xi, & s_{26} &= \frac{L^2}{E}\int_0^1 \frac{\xi}{J(\xi)}d\xi, \qquad \xi = \frac{x}{L}. \end{aligned} \tag{14}$$

Next, we fix displacements at node 1 $\left(\mathbf{d}^{(1)}=\mathbf{0}\right)$ and apply the force $\mathbf{p}^{(2)}$ to node 2. In this case, the internal forces in the beam are

$$\begin{aligned} N(x) &= f_x^{(2)}, & V_y(x) &= f_y^{(2)}, & V_z(x) &= f_z^{(2)}, \\ M_x(x) &= m_x^{(2)}, & M_y(x) &= m_y^{(2)} - f_z^{(2)}(L-x), & M_z(x) &= m_z^{(2)} + f_y^{(2)}(L-x). \end{aligned} \tag{15}$$

The Castigliano theorem with the equilibrium Equation (10) give

$$\mathbf{S}_{22}\mathbf{p}^{(2)} = \mathbf{d}^{(2)}, \qquad \mathbf{p}^{(1)} + \mathbf{R}_{12}\mathbf{p}^{(2)} = \{\mathbf{0}\}, \tag{16}$$

where $\mathbf{S}_{22}$ is the flexibility matrix

$$\mathbf{S}_{22} = \begin{bmatrix} s_{11} & 0 & 0 & 0 & 0 & 0 \\ 0 & s_{22} & 0 & 0 & 0 & \widetilde{s}_{26} \\ 0 & 0 & s_{33} & 0 & -\widetilde{s}_{35} & 0 \\ 0 & 0 & 0 & s_{44} & 0 & 0 \\ 0 & 0 & -\widetilde{s}_{35} & 0 & s_{55} & 0 \\ 0 & \widetilde{s}_{26} & 0 & 0 & 0 & s_{66} \end{bmatrix}, \tag{17}$$

$$\widetilde{s}_{35} = \widetilde{s}_{26} = \int_0^L \frac{L-x}{EJ(x)}\, dx = Ls_{55} - s_{35}.$$

Finally, the blocks of stiffness matrix $\mathbf{K}$ in Equation (9) are defined by the equations

$$\begin{aligned} \mathbf{K}_{11} &= \mathbf{S}_{11}^{-1}, \qquad & \mathbf{K}_{21} &= -\mathbf{R}_{21}\mathbf{K}_{11}, \\ \mathbf{K}_{22} &= \mathbf{S}_{22}^{-1}, \qquad & \mathbf{K}_{12} &= -\mathbf{R}_{12}\mathbf{K}_{22}, \end{aligned} \tag{18}$$

$$\mathbf{K}_{11} = \begin{bmatrix} k_{11} & 0 & 0 & 0 & 0 & 0 \\ 0 & k_{22} & 0 & 0 & 0 & k_{26} \\ 0 & 0 & k_{33} & 0 & -k_{35} & 0 \\ 0 & 0 & 0 & k_{44} & 0 & 0 \\ 0 & 0 & -k_{35} & 0 & k_{55} & 0 \\ 0 & k_{26} & 0 & 0 & 0 & k_{66} \end{bmatrix}, \qquad \mathbf{K}_{12} = \begin{bmatrix} -k_{11} & 0 & 0 & 0 & 0 & 0 \\ 0 & -k_{22} & 0 & 0 & 0 & k_{26} \\ 0 & 0 & -k_{33} & 0 & -k_{35} & 0 \\ 0 & 0 & 0 & -k_{44} & 0 & 0 \\ 0 & 0 & k_{35} & 0 & d_{55} & 0 \\ 0 & -k_{26} & 0 & 0 & 0 & d_{66} \end{bmatrix},$$

$$\mathbf{K}_{21} = \mathbf{K}_{12}^T, \qquad \mathbf{K}_{22} = \begin{bmatrix} k_{11} & 0 & 0 & 0 & 0 & 0 \\ 0 & k_{22} & 0 & 0 & 0 & -\widetilde{k}_{26} \\ 0 & 0 & k_{33} & 0 & \widetilde{k}_{35} & 0 \\ 0 & 0 & 0 & k_{44} & 0 & 0 \\ 0 & 0 & \widetilde{k}_{35} & 0 & k_{55} & 0 \\ 0 & -\widetilde{k}_{26} & 0 & 0 & 0 & k_{66} \end{bmatrix},$$

$$\begin{aligned} k_{11} &= s_{11}^{-1}, & k_{22} &= k_{33} = d_z s_{55}, \\ k_{44} &= s_{44}^{-1}, & k_{55} &= k_{66} = d_y s_{22}, \\ k_{26} &= k_{35} = d s_{26}, & \widetilde{k}_{26} &= \widetilde{k}_{35} = d\widetilde{s}_{26}, \\ k_{55} &= d(Ls_{35} - s_{33}), & k_{66} &= d(Ls_{26} - s_{22}), \end{aligned}$$

$$d = (s_{22}s_{66} - s_{26}^2)^{-1}. \tag{19}$$

By the calculation of the elastic energy of the open-cell structures, there appears a problem of accounting for the elastic energy of the regions of the beam intersections (nodes). The elastic energy of the node regions increases together with the volume concentration of the hard phase of the foams. In this study, we suppose that the nodal force vector $\mathbf{p}$ corresponding to the considered beam does not vary in the node region, and coincides with its value at the point of the beam connections. Let the node have the

coordinate $x = l$ in the local coordinate system, and the characteristic size of the node region be dl. The components of the strain tensor in this region are calculated as follows

$$\varepsilon_{xx} = \frac{\partial u_x}{\partial x} = \frac{N(l)}{ES(l)}, \qquad \gamma_{xy} = \alpha_s \frac{F_y(l)}{\mu S(l)}, \qquad \gamma_{xz} = \alpha_s \frac{F_z(l)}{\mu S(l)}, \tag{20}$$

and the parameters of rotation angle altering are

$$\frac{d\theta_x}{dx} = \frac{M_x(l)}{\mu \widehat{J}_p(l)}, \qquad \frac{d\theta_z}{dx} = \frac{M_y(l)}{EJ(l)}, \qquad \frac{d\theta_y}{dx} = \frac{M_z(l)}{EJ(l)}. \tag{21}$$

Using these equations one can determine the corresponding part of the energy by integrating Equation (20) and Equation (21) along the dl element. If the ligament is very short ($L < 2dl$) , it is considered to be a beam of a constant cross-section. Note that the accepted geometrical model of the ligament (Section 2) allows us to calculate all the integrals in the above equations in closed analytical forms.

If the stiffness matrices of all the beam elements are constructed, the final system of the EFM may be obtained by the displacement method [Cook et al. 1989]. This system follows from the conditions that the displacement vectors of the beam ends connected at one node are the same for all these beams.

5. Representative volume element of the open-cell foam materials

Let us go to the calculation of the effective elastic properties of the foam material. The procedure of simulation of the foam microstructure inside a cubic region, V described in Section 2, give us the skeleton of the foam microstructure inside the RVE: the coordinates of the nodes and the rule of their connections by the ligaments. The parameters of the ligaments mentioned in Section 3 are the other part of information necessary for performance of the EFM calculations. The version of the EFM considered in the previous section is used to calculate displacements, angles of rotations, forces and moments at all the nodes of the beam structure by the prescribed boundary conditions on the surface of the RVE (cube V). Note that the ligaments that are placed on the surface of cube V should be deleted from the skeleton in order to obtain reliable values of the effective elastic constants of the foam material. These ligaments appear as a result of the mirror reflections of the seed point inside V with respect to the sides of the cube (see Section 2). They don't correspond to the actual foam structure and provoke excess of rigidity of the considered RVE.

In the nodes that are on the surface Ω of the cube V one has to define static and kinematic conditions that are necessary for uniqueness of the solution of the elasticity problem. Let us define the components of the displacement vector $u_i^{(k)}$ at the surface nodes $x^{(k)}$ ($x^{(k)} \subset \Omega$) by the following equation (affine deformation)

$$u_i^{(k)} = \varepsilon_{ij} x_j^{(k)}, \tag{22}$$

where ε_{ij} is a fixed symmetric tensor. All angles of rotations of the surface nodes are assumed to be equal to zero. These boundary conditions are sufficient in order to obtain displacements, forces and moments at every node of the beam structure including the border nodes.

Let us go to the homogenization problem that is the determination of a homogeneous elastic material equivalent to the given foam material. It means that the elastic module tensor C^* of the equivalent material should coincide with the tensor that connects the mean values of the stress $\langle \sigma_{ij} \rangle$ and strain $\langle \varepsilon_{ij} \rangle$

tensors over the RVE of the foam material

$$\langle \sigma_{ij} \rangle = C^*_{ijkl} \langle \varepsilon_{kl} \rangle , \tag{23}$$

$$\langle \sigma_{ij} \rangle = \frac{1}{V} \int\limits_V \sigma_{ij}(x) dv, \qquad \langle \varepsilon_{ij} \rangle = \frac{1}{V} \int\limits_V \varepsilon_{ij}(x) dv. \tag{24}$$

Let us consider a volume of the equivalent homogeneous material that coincides with the RVE and is loaded with the forces $f_j(x) = n_k(x)\sigma_{kj}(x)$ on its surface Ω. Here $\sigma_{kj}(x)$ is the stress tensor, n_i is the external normal to Ω . The surface integral

$$\int\limits_\Omega f_j(x) x_i d\Omega$$

may be transformed in a volume integral using the Gauss theorem as follows

$$\int\limits_\Omega f_j(x) x_i d\Omega = \int\limits_\Omega n_k(x)\sigma_{kj}(x) x_i d\Omega = \int\limits_V \partial_k \left[\sigma_{kj}(x) x_i\right] dv = \int\limits_V \left[\partial_k \sigma_{kj}(x)\right] x_i dv + \int\limits_V \sigma_{ij}(x) dv.$$

Because of the equilibrium equation for the stress tensor $\sigma_{kj}(x)$ $\left(\partial_k \sigma_{kj}(x) = 0\right)$, the first integral in the right hand side of this equation disappears, and for the mean stress field $\langle \sigma_{ij} \rangle$ over the cube V we obtain

$$\langle \sigma_{ij} \rangle = \frac{1}{V} \int\limits_V \sigma_{ij}(x) dv = \frac{1}{V} \int\limits_\Omega f_j(x) x_i d\Omega. \tag{25}$$

It follows from this equation that in the case of the beam structure, the mean stress tensor inside the cubic RVE may be calculated as follows

$$\langle \sigma_{ij} \rangle = \frac{1}{8} \sum_{x^{(k)} \subset \Omega} F^{(k)}_j x^{(k)}_i, \tag{26}$$

where $F^{(k)}_j$ is the vector of the concentrated force acting in the surface node $x^{(k)}$. It is taken into account that the volume of the cube V is equal to 8.

For the affine surface deformation Equation (22), the mean strain tensor $\langle \varepsilon_{ij} \rangle$ defined in Equation (24) coincides with the tensor ε_{ij} presented in boundary conditions Equation (22). Thus, using (23) and (26) one can calculate the components of the tensor C^*_{ijkl} (tensor of the effective elastic modules) if the forces $F^{(k)}_j$ in the surface nodes are obtained from the solution of the elasticity problem for the considered beam structure.

Application of other boundary conditions on the surface of the cube V faces additional computational difficulties. For instance, one can define the forces $F^{(k)}_j$ and the moments at all the surface nodes and calculate the mean strain tensor from Equation (26). For a homogeneous material, the mean strain field defined in Equation (24) may be transformed in a surface integral

$$\langle \varepsilon_{ij} \rangle = \frac{1}{V} \int\limits_V \varepsilon_{ij}(x) dv = \frac{1}{V} \int\limits_\Omega n_{(i}(x) u_{j)}(x) d\Omega. \tag{27}$$

Here $\varepsilon_{ij}(x) = \partial_{(i}u_{j)}(x)$, $u_i(x)$ is the displacement vector, parentheses in indices mean symmetrization. Thus, for calculation of the mean strain field one has to calculate the integral in the right hand side of Equation (27) from the solution of the elasticity problem for the beam structure. Note that the FEM provides the values of displacements u_j only in a finite number of the surface nodes. Thus, in order to find the mean strain field $\langle\varepsilon_{ij}\rangle$ from Equation (27), one has to interpolate function $u(x)$ on all the points of surface Ω, and after that, to calculate the surface integral in the right hand side of Equation (27) numerically. Such interpolation and integration are sources of additional numerical errors that cannot be avoided if the force boundary conditions on Ω are used.

Very often in the literature, for the numerical solution of the homogenization problems, periodic boundary conditions on the surface of the RVE are applied. Note that for the cubic volume element discussed in Section 2, such conditions cannot be imposed. In the framework of the beam FEM, the periodic conditions are to be formulated in a finite number of surface nodes. But the position of the nodes on the opposite sides of cube V are not symmetric, and strictly speaking, the periodic boundary conditions cannot be formulated. On the other hand, one can consider a tesselation process using not mirror but periodic continuation of the seed points $S_{(0,0,0)}$ inside the cube V on all three-dimensional space. In this case, the Voronoii or Laguerre polyhedra corresponded to the original seed point set $S_{(0,0,0)}$ inside V will compose not a cubic region, but a region with a rather complex, nonplane surface. The calculation of the mean strain field over such a region using Equation (27) faces an additional difficulty of definition of the external normal $n(x)$ at all the points of such a surface. The latter contains many angle points where normals are not defined. Note that the displacement vectors are calculated at the nodes that are the vertices of the polyhedra. Thus, for the calculation of the mean strain field over the region V, one has to interpolate the displacement field onto all points of a nonplane surface Ω, and then to calculate the integral in the right hand side of Equation (27) numerically. Both operations are connected with some numerical errors. That is why in this study, only kinematic boundary conditions (22) are considered.

Let us go to the problem of definition of the number N of cells inside the RVE that are sufficient to obtain reliable values of the effective elastic constants of the foam material. In the series of numerical experiments, the Voronoii tessellation procedure was used for generation of the foam microstructures. The seed points were independently and homogeneously distributed inside the cube by the condition that these points cannot be closer than a distance h from each other. The distance h was chosen in order to generate the set of seed points in a reasonable time. Circular, cylindrical, ligaments with parameters: $a_1 = 100, a_3 = 0$ were considered; parameter a_2 depends on the volume concentration of the hard phase. The material of the ligaments was taken to be isotropic with the Young modulus E and the Poisson ratio $\nu = 0.3$.

We have considered the increasing number of the cells from one hundred to fifteen hundreds. For the calculation of the effective elastic moduli, the following six different kinematic boundary conditions were used. Extension of the cube in the direction of x_1, x_2 or x_3-axes ($\varepsilon_{ij}^{(1)} = \delta_{1i}\delta_{1j}$, $\varepsilon_{ij}^{(2)} = \delta_{2i}\delta_{2j}$, $\varepsilon_{ij}^{(3)} = \delta_{3i}\delta_{3j}$), and three independent shear deformations on the cube surface:

$$\varepsilon_{ij}^{(4)} = \delta_{1(i}\delta_{2j)}, \qquad \varepsilon_{ij}^{(5)} = \delta_{1(i}\delta_{3j)}, \qquad \varepsilon_{ij}^{(6)} = \delta_{2(i}\delta_{3j)}.$$

We calculate the effective elastic Young and shear moduli in the directions of the coordinate axes for the increasing number of the cells inside V. We also evaluate anisotropy of the effective moduli with respect to tension and shear deformations. Because for an isotropic material, the Young E_* and shear μ_* moduli

are connected by the equation

$$\mu_* = \frac{E_*}{2(1+\nu_*)}, \tag{28}$$

one can introduce anisotropy parameter α defined by the equation

$$\alpha = \frac{2(1+\nu_*)\mu_*}{E_*}, \tag{29}$$

and the closer to 1 the value of α, the closer to isotropy the symmetry of the tensor of the effective elastic moduli C^* of the cubic RVE.

Another parameter β

$$\beta = \frac{1}{\langle E_* \rangle}\sqrt{\langle (E_* - \langle E_* \rangle)^2 \rangle} \tag{30}$$

characterizes the dispersion of the effective Young modulus over the realizations of the foam structures. Here the average is taken over three directions and over the realizations of the random microstructures for a fixed number of cells inside the RVE.

In Figures 10, 11, and 12, the dependences of the reduced effective Young E_R and shear μ_R moduli of the RVE on the number N of cells inside the RVE are presented. The reduced moduli are defined by the equations

$$E_R = \frac{E_*}{p^2 E}, \qquad \mu_R = \frac{\mu_*}{p^2 \mu}, \qquad p = \frac{\rho_*}{\rho}. \tag{31}$$

Here E, μ, ρ are the Young modulus, shear modulus, and density of the foam hard phase, ρ_* is the density of the foam, p is the volume concentration of the hard phase. The graphs in Figure 10 correspond to the volume concentration of the hard phase $p = 0.01$, in Figure 11 to $p = 0.05$, and in Figure 12 to $p = 0.1$.The same dependences for the Poisson ratio ν_* are presented in Figure 13. Dependences of the anisotropy coefficient α and dispersion coefficient β on the number N of cells in the RVE are in Figures 14 and 15 for $p = 0.01$. The vertical bars in these figures show the dispersions of the numerical results

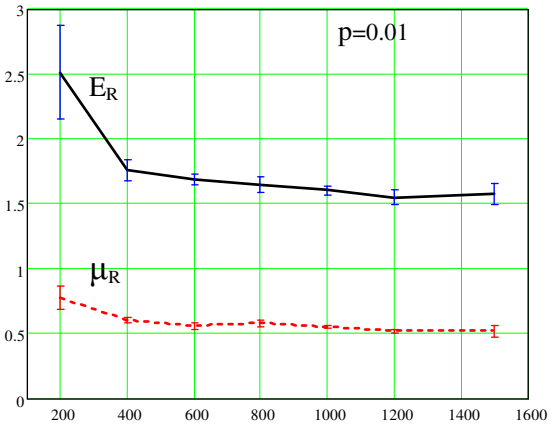

Figure 10. The dependences of the reduced Young E_R and shear μ_R moduli (Equation (31)) on the number N of cells in the RVE for the volume concentration of the hard phase $p = 0.01$.

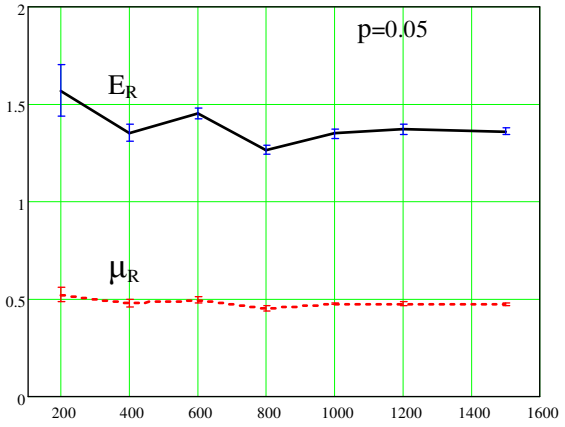

Figure 11. The same graphs as in Figure 10 for $p = 0.05$.

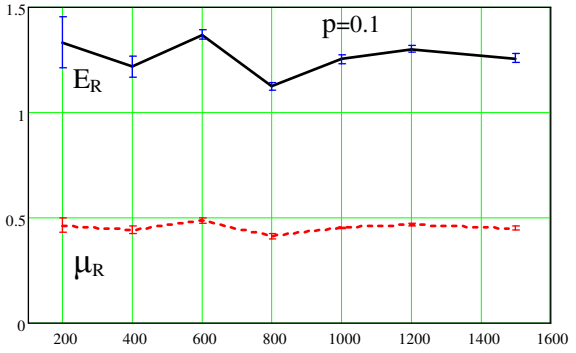

Figure 12. The same graphs as in Figure 10 for $p = 0.1$.

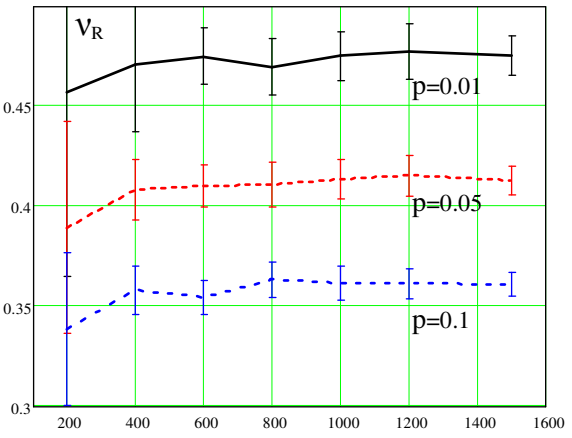

Figure 13. The dependence of the Poisson ratio ν_* of the foam on the number N of cells in the RVE.

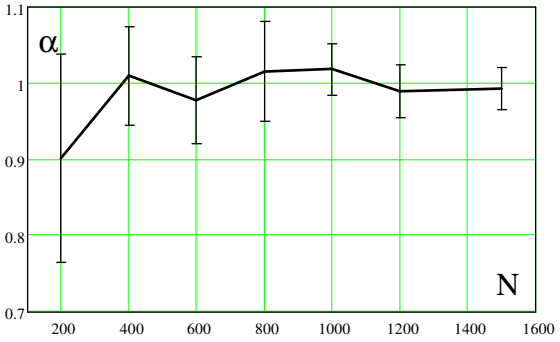

Figure 14. The dependence of the isotropy parameter α (Equation (29)) on the number N of cells in the RVE, $p = 0.01$.

among the realizations of the microstructures with fixed values of the cell number N. For every value of N, 5–7 realizations of the random structures were taken.

The main conclusion that can be made up from these graphs is that the RVE should contain about 900–1000 cells in order to obtain reliable values of the effective elastic properties of the open-cell foam materials. For such a number of cells in the RVE ($N = 1000$), the dependences of the relative effective Young modulus E_*/E of the foams on the volume concentration p of the hard phase are presented in Figure 16. Square points in this figure are experimental data of Gibson and Ashby [1982], triangle points are the data of Liderman [1971], and circles are the data of Hagiwara and Green [1987] . The line with black dotes is the result of our simulations for the foam with circular cylindrical ligaments ($a_1^{-1} = 0$), and the line with black triangles corresponds to the foams with triangle cylindrical ligaments ($a_1^{-1} = 0.5$). Note that the detailed information about the ligament shapes is absent in the mentioned experimental works.

If the number of cells inside the RVE is taken smaller than indicated above, dispersion of the numerical values of the effective elastic constants for different realizations of the foam microstructures increases (Figure 15). It is necessary also to emphasize that the mean value of these constants over the realizations

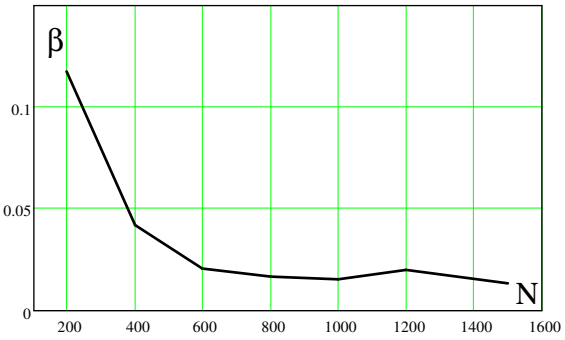

Figure 15. The dependence of the dispersion coefficient β of the effective Young modulus (Equation (30)) on the number N of cells in the RVE, $p = 0.01$.

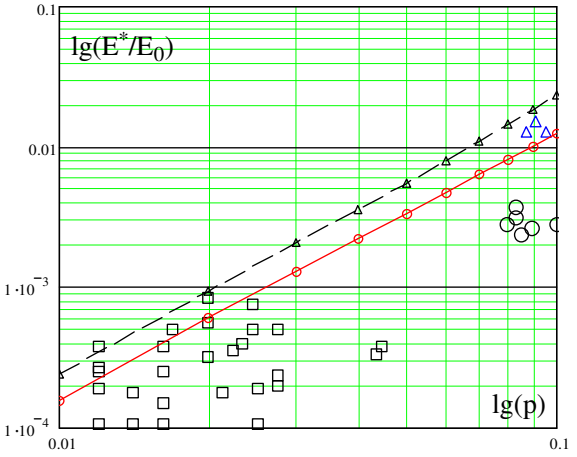

Figure 16. The dependences of the relative effective Young modulus (E_*/E) on the volume concentration p of the hard phase of the foam. Triangle points correspond to the data from [Liderman 1971]; square points from [Gibson and Ashby 1982]; circle points from [Hagiwara and Green 1987]; the line with dots are theoretical predictions for the foams with circular cylindrical ligaments ($a_1^{-1} = 0$, $a_3 = 0$), the line with triangles is the prediction for triangular cylindrical ligaments $a_1^{-1} = 0.5$, $a_3 = 0$).

does not coincide with the mean values of the constants for the RVE with a sufficiently large number of cells (Figure 16). The same fact was noted in [Kanit et al. 2003], where the problem of the appropriate size of the RVE for random polycrystalline materials was considered.

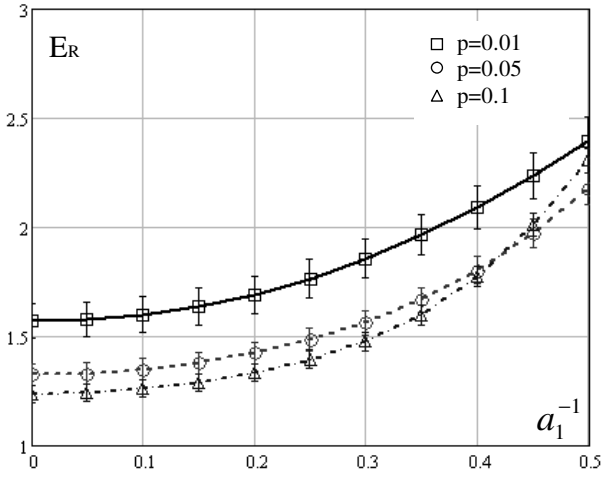

Figure 17. The dependence of the reduced effective Young modulus E_R on the shape of the cross-section (parameter a_1) for cylindrical ligaments $a_3 = 0$.

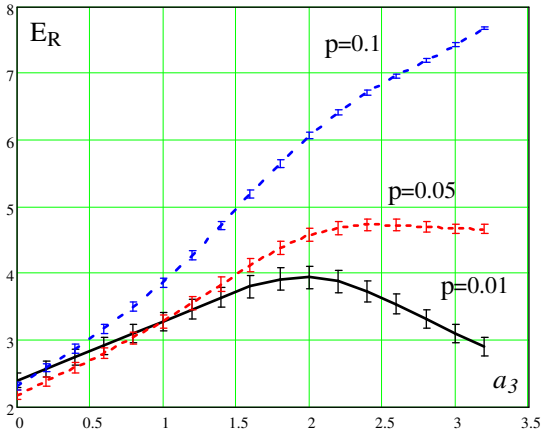

Figure 18. The dependence of the reduced effective Young modulus E_R on the ligament axial altering (parameter a_3) for triangle ligaments ($a_1^{-1} = 0.5$).

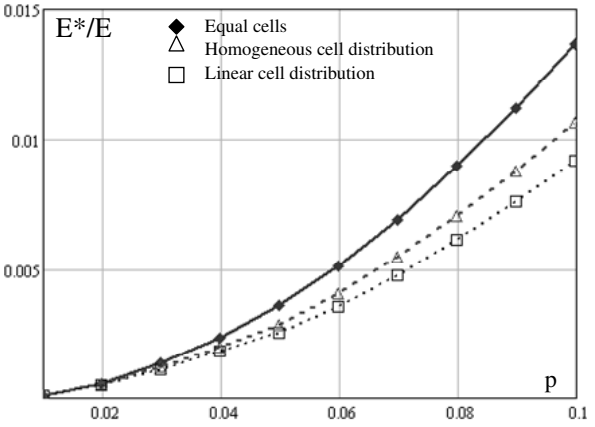

Figure 19. The dependences of the relative effective Young modulus (E_*/E) on the law of distribution of cell diameters and the volume concentration p of the hard phase for the foams with circular cylindrical ligaments ($a_1^{-1} = 0, a_3 = 0$). The line with black rhombs correspond to approximately equivalent cell diameters, the line with triangles to a homogeneous distribution of cell diameters, and the line with squares to a linear distribution of the diameters.

6. Dependences of elastic properties of open-cell foams on the ligament shapes and the law of the cell size distribution

The effective Young moduli of the foams with ligaments of various shapes were calculated according to the proposed algorithm. The results of such calculations are presented in Figures 17 and 18. As it was indicated in Section 2, the parameter a_1 $(0 < a_1^{-1} < 0.5)$ describes the shape of the cross-sections of the ligament, and parameter a_3 defines the altering of the ligament cross-section along its axis $(0 < a_3 < 4,$

$a_3 = 0$ corresponds to a cylindrical ligament). As it is seen from these graphs, the reduced Young modulus E_R is more sensitive to the parameter a_3 altering than to altering the parameter a_1.

The dependences of relative Young modulus E_*/E of the foams on the distribution of cell diameters inside the RVE and on the volume concentration p of the hard phase are presented in Figure 19. In this figure, the line with black rhombs corresponds to the foams with almost equal diameters of the cells (the distribution function of the cell diameters is presented in Figure 6 also by the line with black rhombs), the line with triangles corresponds to the homogeneous distribution of cell diameters in the interval $(0.5\,\langle d\rangle\,,\,1.5\,\langle d\rangle)$, and the line with squares correspond to the linear distribution of the cell diameters in the interval $(0.3\,\langle d\rangle\,,\,1.2\,\langle d\rangle)$ (the corresponding distribution functions are in Figure 6). As it is seen from these graphs, for a fixed volume concentration of the hard phase, the foams with a wide distribution of cell diameters have lower elastic modules than the foams with approximately the same diameters of cells.

7. Conclusion

This work proposes a method of calculating the effective elastic properties of open-cell foam materials in two stages: simulation of the microstructure of the foam inside a RVE of such a material, and application of a specific version of the FEM for the calculation of stresses and stains in the ligaments of the foam structure. The Laguerre tesselation algorithm adapted in this work allows us to simulate the foam microstructures with any prescribed cell size distribution law. But this algorithm is more complex than the conventional Voronoii algorithm. It requires carrying out the procedure of close packing of spheres with the given distribution of the diameters inside the RVE. The coordinates of the centers of the spheres obtained after the packing, and the diameters of the spheres associated with every center, are initial data for the Laguerre tesselation process.

The size of the RVE is a crucial problem for the numerical simulation of the properties of the open-cell foams. As is shown in this work, the size of the RVE, or the minimal number N of the calls inside the RVE that is necessary to obtain reliable values of the effective elastic constants, depends on the volume concentration p of the hard phase. For small volume concentrations ($p = 0.01$) this number turns out to be about 900–1000, and the value of N decreases when p increases: N is about 800 for $p = 0.05$, and about 400 for $p = 0.1$.

The influence of the form of the ligaments on the effective elastic properties is essential, but altering the ligament cross sections along the ligament axes affects the values of the effective elastic moduli more strongly than altering the shape of the cross sections.

The influence of the cell diameter distributions on the effective elastic properties of the foams is also notable. For the foams with a wide distribution of cell diameters, the effective Young moduli turn out to be less than the modules of the foams with approximately equal cells, and the difference grows with the volume concentration p of the hard phase. It was also indicated that for the same volume concentration of the hard phase, the foams with a linear distribution of cell diameters have lower Young moduli than the foams with homogeneous distribution of cell diameters.

Acknowledgement

The authors thank Dr. Ozden Ochoa, Dr. Khalid Lafdi, and Dr. Dominique Jeulin for fruitful discussions.

References

[Aurenhammer and Klein 2000] F. Aurenhammer and R. Klein, "Voronoi diagrams", pp. 201–290 in *Handbook of computational geometry*, edited by J.-R. Sack and J. Urrutia, Elsevier, Amsterdam, 2000.

[Christensen 2000] R. M. Christensen, "Mechanics of cellular and other low density materials", *Int. J. Solids Struct.* **37**:1-2 (2000), 93–104.

[Cook et al. 1989] R. D. Cook, D. S. Malkus, and M. E. Plesha, *Concepts and applications of finite element analysis*, 3rd ed., Wiley, New York, 1989.

[Gibson and Ashby 1982] L. J. Gibson and M. F. Ashby, "The mechanics of three dimensional cellular materials", *P. Roy. Soc. Lon. A Mat.* **382**:1782 (1982), 43–59.

[Gong et al. 2005] L. Gong, K. S., and J. W.-Y., "Compressive response of open-cell foams, I: Morphology and elastic properties", *Int. J. Solids Struct.* **42**:5-6 (2005), 1355–1378.

[Hagiwara and Green 1987] H. Hagiwara and D. J. Green, "Elastic behavior of open-cell alumina", *J. Am. Ceram. Soc.* **70**:11 (1987), 811–815.

[Kadashevich and Stoyan 2005] I. Kadashevich and D. Stoyan, "Micro-mechanical analysis of ACC", pp. 219–228 in *Autoclaved aerated concrete*, Taylor and Francis, London, 2005.

[Kanit et al. 2003] T. Kanit, S. Forest, I. Galliet, V. Mounoury, and D. Jeulin, "Determination of the size of the representative volume element for random composites: statistical and numerical approach", *Int. J. Solids Struct.* **40**:13-14 (2003), 3647–3679.

[Liderman 1971] J. M. Liderman, "The prediction of the tensile properties of flexible foams", *J. Appl. Polym. Sci.* **15**:3 (1971), 693–703.

[Pilkey et al. 2003] W. D. Pilkey, , and W. Wunderlich, *Mechanics of structures, variational and computational methods*, 2nd ed., CRC Press, Boca Raton, FL, 2003.

[Roberts and Garboczi 1999] A. P. Roberts and E. J. Garboczi, "Elastic properties of a tungsten-silver composite by reconstruction and compilation", *J. Mech. Phys. Solids* **47**:10 (1999), 2029–2055.

[Roberts and Garboczi 2001] A. P. Roberts and E. J. Garboczi, "Elastic properties of model random three-dimensional closed-cell cellular solids", *Acta Mater.* **49**:2 (2001), 189–197.

[Roberts and Garboczi 2002] A. P. Roberts and E. J. Garboczi, "Elastic properties of model random three-dimensional open-cell solids", *J. Mech. Phys. Solids* **50**:1 (2002), 33–55.

[Tenemura et al. 1983] M. Tenemura, T. Ogawa, and N. Ogita, "A new algorithm for three-dimensional voronoi tessellation", *J. Comput. Phys.* **51**:2 (1983), 191–207.

[Warren and Kraynik 1997] W. E. Warren and A. M. Kraynik, "Linear behavior of a low-density kelvin foam with open cells", *J. Appl. Mech.* (*Trans. ASME*) **64** (1997), 787–793.

[Zhu et al. 2000] H. X. Zhu, J. R. Hobdell, and A. H. Windle, "Effect of cell irregularity on the elastic properties of open-cell foams", *Acta Mater.* **48**:20 (2000), 4893–4900.

Received 19 Jun 2006. Accepted 8 May 2007.

SERGEY KANAUN: kanaoun@itesm.mx
Departamento de Ingenieria Mecánica, Instituto Tecnológico y de Estudios Superiores de Monterrey, Campus Estado de México, Carretera Lago de Guadalupe 4 km Atizapan, Edo de México, 52926, Mexico

OLEKSANDR TKACHENKO: oleksandr.tkachenko@itesm.mx
Departamento de Ingenieria Mecánica, Instituto Tecnológico y de Estudios Superiores de Monterrey, Campus Estado de México, Carretera Lago de Guadalupe 4 km Atizapan, Edo de México, 52926, Mexico